2010 IEEE International Conference on Robotics and Automation
Anchorage Convention District
May 3-8, 2010, Anchorage, Alaska, USA

Robotic Delivery of Complex Radiation Volumes for Small Animal Research

Mohammad Matinfar†, Iulian Iordachita§, John Wong‡ and Peter Kazanzides†

†Dept. of Computer Science, Johns Hopkins Univ., Baltimore, MD [bmat,pkaz@jhu.edu]
‡ Dept. of Radiation Oncology, Johns Hopkins Medical Inst., Baltimore, MD
§ Dept. of Mechanical Engineering, Johns Hopkins Univ., Baltimore, MD

Abstract— **The Small Animal Radiation Research Platform (SARRP) is a novel and complete system capable of delivering multidirectional (focal), kilo-voltage radiation fields to targets in small animals under robotic control using cone-beam CT (CBCT) image guidance. The capability of the SARRP to deliver highly focused beams to multiple animal models provides new research opportunities that more realistically bridge laboratory research and clinical translation. This paper describes the design and operation of the SARRP for precise radiation delivery. Different delivery procedures are presented which enable the system to radiate through a series of points, representative of a complex shape. A particularly interesting case is shell dose irradiation, where the goal is to deliver a high dose of radiation to the shape surface, with minimal dose to the shape interior. The ability to deliver a dose shell allows mechanistic research of how a tumor interacts with its microenvironment to sustain its growth and lead to its resistance or recurrence.**

I. Introduction

The deployment of advanced technologies and the translation of laboratory discoveries for human treatment must be supported by rigorous pre-clinical studies. Pre-clinical studies of new radiation treatment methods, however, have been difficult due to the technological disparity between the simple methods for laboratory animal irradiation and those for advanced human treatment. Recognition of this deficiency has led us [1] and other investigators [2]–[5] to develop specialized radiation delivery systems with a precision that is suitable for laboratory mice and rats. A common goal of these systems is to deliver irradiation to a localized region in the mouse. The scale of the problem can be appreciated when one considers that the brain of the mouse, for example, is approximately 1 cm wide and structures of interest within the brain are much smaller than that, often less than 1 mm in at least one dimension.

The SARRP is designed to deliver precision radiation beams as small as 0.5mm in diameter. It has computer controlled robotic translation and rotation stages that move an animal subject during radiation, and an x-ray tube mounted on a rotating gantry assembly that allows the user to direct a beam from various angles over a 120° arc. The SARRP is equipped with a flat panel amorphous silicon detector for CBCT imaging, which is obtained by rotating the animal while acquiring multiple projection images.

One approach to treatment planning is to create a shell of dose around the cancerous tissue to disjoin it from its surrounding biological structures. This approach's main utility is to enable laboratory experiments to test the much disputed hypothesis that, at high doses, tumor control is driven by damage to the tumor vascular supply and not by damage to the tumor cells themselves. There is new evidence that bone marrow derived cells can reconstitute tumor blood vessels in mice after irradiation [6]. The main challenge in this approach is to create an appropriate dose shell that has enough strength to cut out the supplying blood-vessels. We introduce an approach, motivated by solid geometry, to create a dose shell. Creating a sphere from the intersection of cylinders is a well-known mathematical problem and it is shown that the intersection of a large enough number of cylinders is a sphere. Moreover, it has been shown that circumsolids (solid 3-D shapes that circumscribe spheres) could be generated from a class of building blocks, such as conical-faced shapes [7]. Finally, we introduce a routine to utilize the pencil beam to create the contours of a complex shape from different beams eye views, corresponding to different gantry angles. The routine is demonstrated by extracting and painting dose on the projection of the left lateral ventricle of a mouse brain.

II. Mechanics

Figure 1 highlights the components of the second generation SARRP. The system comprises a constant-voltage, dual-focus (0.4 and 3 mm spot sizes), 225 kVp source mounted on a rotating isocentric gantry. The gantry is driven by a motor from 0° at vertical to 120°. The gantry isocenter is set at 35 cm from the x-ray focal spot. The motorized gantry improves the accuracy of the system over the manual gantry rotation (first generation SARRP [1]) and provides a continuous motion of gantry over the 120° arc. A set of robotic stages provides four degrees of freedom (x, y, z and a rotational motion), used in positioning the animal. The combination of gantry orientation and robotic stage motion facilitates the delivery of complex conformal dose distributions. A radiosurgery-like collimating "nozzle" system is employed to rigidly align with the x-ray source and output small radiation fields. Radiation beams with dimensions ranging from 0.5 mm in diameter to 200×200 mm are delivered with regularly and irregularly shaped collimators or blocks. Filtration is used to remove the low-energy contamination in

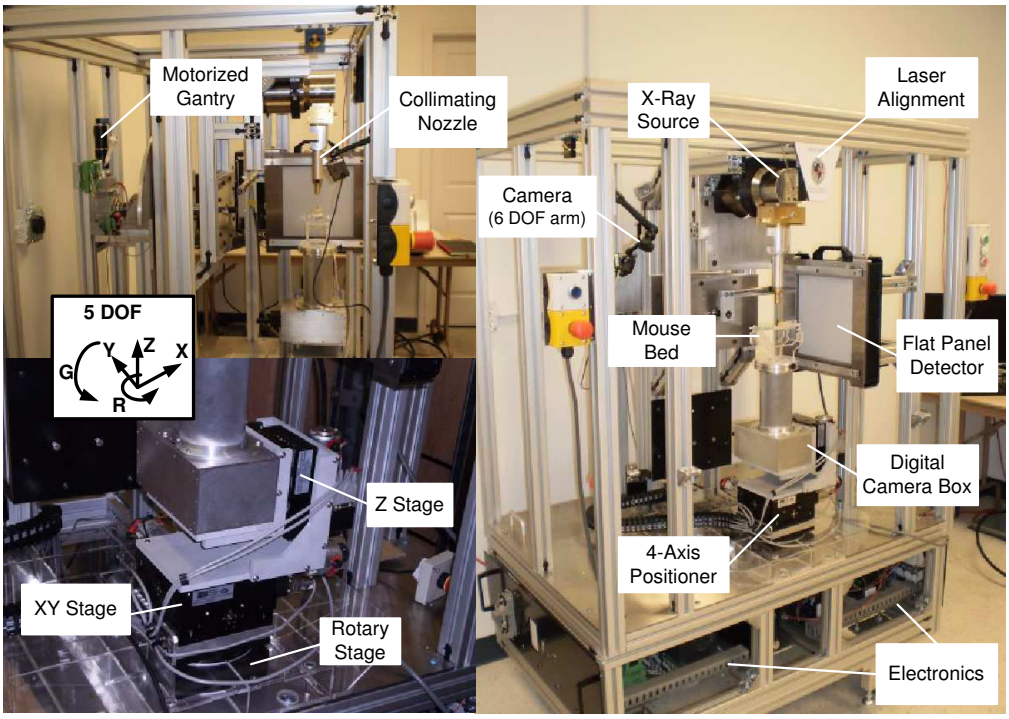

Fig. 1. Different components of the second generation SARRP, showing a 5 degrees of freedom (DOF) manipulator

the x-ray spectrum. The SARRP provides a laser alignment system to facilitate accurate, reproducible setup of subjects. This enables visual setup of large treatment fields, where an accuracy of several millimeters is sufficient.

III. Calibration of Delivery Beam

Radiation treatment is often delivered from multiple poses that are intended to intersect at a specified point (the isocenter). Using beams from multiple angles results in a confined dose distribution that limits dose to surrounding areas. With the SARRP, rotation about a target can be obtained via the rotary axis or the x-ray gantry. In reality, there is no single isocenter because the two axes of rotation do not (in general) intersect and even if they did, physical factors such as gravity loading on the mechanical structure would cause the x-ray beam to deviate from its ideal positions. Thus, x-ray beams delivered from multiple gantry angles will not intersect at a single point. One common solution is to find a single "best-fit" isocenter, but this approach does not yield sufficient accuracy for our system. Our solution is to make the isocenter a function of the gantry angle – as the gantry rotates, the robotic stages move the target so that it remains in the path of the radiation beam.

We developed a calibration procedure that uses an x-ray camera, mounted on the robotic stages, to determine the location of the beam axes for specific gantry angles, as described in [8]. Briefly, a collimator is attached so that the x-ray produces a bright spot on the camera image. To eliminate the requirement for camera calibration, we use visual servoing to move the robot stages until they center the

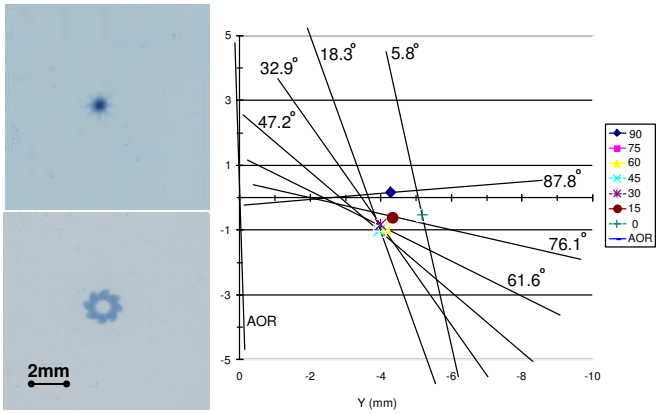

Fig. 2. 0.5 mm uncalibrated (left-bottom) and calibrated (left-top) beam over 360° arc at isocenter for gantry at 45° - Digitally constructed "star shot" showing x-ray beams for each gantry angle (right). Plot shows both nominal gantry angles (right-most table) and measured angles (on each line), AOR=Axis of rotation, other symbols indicate gantry-specific isocenter.

x-ray spot at a specific pixel. The direction of the beam axis is determined by performing this procedure at two distinct regions of the workspace. Once the location of each beam axis is determined, the following least-squares estimation problem is solved to identify the point on each beam axis that is closest to the nominal isocenter:

$$\min \sum_{\phi} \|P(\phi) + D(\phi)s(\phi) - C\|^2 \qquad (1)$$

where $P(\phi)$ and $D(\phi)$ are the (measured) point and direction

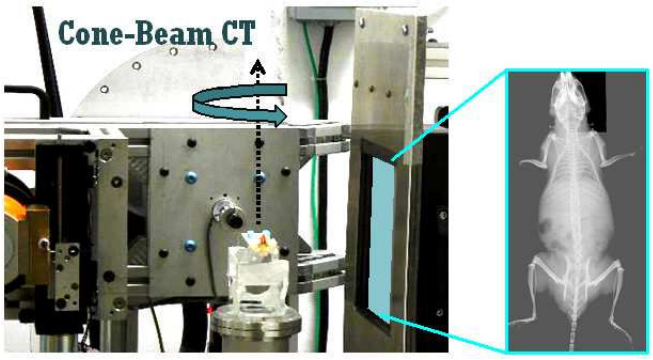

Fig. 3. Configuration for cone-beam CT on small animal

Fig. 4. The interface of the XVI software used for cone-beam CT reconstruction and visualization

vector that define the beam axis at the gantry angle ϕ, C is the (unknown) nominal isocenter, and $s(\phi)$ is the (unknown) parameter that defines the point on the line that is closest to C. Thus, for each gantry angle ϕ, the gantry-specific isocenter is given by $P(\phi)+D(\phi)s(\phi)$.

The result of calibration is shown in Figure 2. Seven distinct gantry positions are chosen for calibration and the isocenter for each position is found. The beam along each gantry angle and the corresponding isocenter is constructed digitally and depicted in Figure 2-right. This figure shows that a single best-fit isocenter would not produce the sub-millimeter accuracy required for small animal experiments. Our calibration method is based on the premise that higher accuracy can be achieved by defining multiple isocenters and moving the robotic positioner to place the target at the appropriate isocenter. Figure 2-left compares an uncalibrated beam and calibrated beam when the beam is delivered over a 360° arc at isocenter for gantry at 45° [8].

IV. Image Guidance System

Several of the new small animal radiation systems are equipped with on-board CT guidance to facilitate precise positioning in repeat irradiation experiments [2], [3]. Such capability parallels the on-line image guidance technologies in human treatment, including cone-beam CT (CBCT), which are supplanting the traditional reliance on custom immobilization devices to set up each patient. Clearly, on-board imaging is advantageous for human applications to monitor the inherent motion of the un-sedated patient, and in the case of CBCT, to provide information about soft tissue targets. CT-guidance is necessary to ensure high precision repeat irradiation even when the anesthetized animal is immobilized. As a corollary, on-board image guidance ensures accurate irradiation, alleviating the concern of inadequate animal immobilization.

On-board CBCT imaging is achieved by a 360^o rotation of the horizontal animal between the stationary x-ray source and a 20 cm x 20 cm flat-panel detector (Perkin Elmer, Santa Clara, CA). This approach was chosen as the most direct method to accommodate the robotic stages for positioning the animal for complex irradiation arrangements. The flat panel has 1024 × 1024 pixels and is placed at 17.5 cm from the isocenter to attain an image magnification factor of 1.5, resulting in a pixel dimension of 0.13 mm × 0.13 mm at isocenter. Dark current and gain correction images are acquired prior to each imaging run and used to correct pixel intensities as each image is acquired. Figure 3 shows the configuration of the CBCT scanning orientation and the resultant 100 kVp image of a mouse. The CT imaging dose is less than 1 cGy using 100 kVp x-rays.

Aside from on-board cone-beam CT, the SARRP is equipped with a secondary imaging system. Oriented orthogonal to the flat-panel imaging system is a digital fluoroscopic camera box used for taking anterio-posterior (or vice versa) radiographs, to be potentially used in conjunction with lateral radiographs from the flat panel detector. This imaging capability was developed for experiments not requiring CBCT-based image guidance. Simple setup verification can be obtained from these orthogonal projection images.

Volumetric reconstruction is accomplished using filtered back projection [9]. The imaging software is the XVI platform from the Netherlands Cancer Institute (NKI) [10]. The interface is shown in Figure 4. The marker in the sagittal image locates the target and the coordinates of that point are written to a file, which is then parsed by the SARRP software. Because the imaging coordinate system is registered to the robot coordinate system, the software can convert the CBCT coordinates of the target to robot coordinates, and subsequently command the robot to move the target to the isocenter.

V. Delivery Procedures

Radiotherapy planning mainly addresses the calculation of the dose distribution at the target for a given treatment technique. Treatment set-ups are determined to optimize the beam configurations such that a specified dose distribution is delivered to the target volume. In general, a grid is superimposed on an image (e.g. CT) of a cross-section of

the patient and the oncologist identifies the planning target volumes (PTV) and the organs at risk (OAR) [11]. For pixels in the PTVs the total deposited dose must be above a lower bound and for the pixels in the OARs the total deposited dose must be less than an upper bound. Since the contributed dose is a linear combination of the intensities carried by the individual beams, the problem of treatment planning becomes a linear feasibility problem.

A. Dose Painting Procedure

The dose painting procedure extends the functionality of the system by enabling it to radiate through a series of points, representative of a complex shape with large kinks and curvatures. Localized radiation to this complex trajectory path, allows for precise irradiation. As compared to whole tissue radiation therapy, dose painting will minimize radiation exposure to healthy surrounding tissue in an accurate and efficient manner. The SARRP's ability to deliver radiation from multiple gantry angles and at the same time moving the target with four degrees of freedom, enables the dose painting of 3-D targets while avoiding critical structures. Further details are reported in [12].

B. Peripheral Dose Distribution

One of the theories of peripheral (shell) dose distribution is to preferentially deliver dose to the most critical biological region, the tumor periphery, where invasion and most rapid growth occurs. Relatively large tumors reach a stage where the radiation dose to the total tumor must be limited due to acute life threatening toxicity. The total volume integral dose to the tumor can be reduced if only the tumor periphery is irradiated to a high dose. The theory also proposes that eradicating viable vasculature at the periphery of a tumor will limit the growth potential of tumor cells at the tumor core.

Dose, like temperature, is a quantity that can be attached to each point of an irradiated body [13]. The principle underlying shell dose distribution is that the intensity map of the incident beam could be drawn over the shell of the target 3-D structure. We propose a treatment planning approach that is motivated by solid geometry. The intersection of two (or three) right circular cylinders of equal radii is called the Steinmetz solid. This solid is shown in Figure 5. For two cylinders of radius r along the Z and X axes (the planes spanned by the XY and YZ robot stages), the surface area can be found as $\int x ds$, where

$$ds = \sqrt{1+(\frac{dy}{dz})^2}\, dz = \frac{r}{\sqrt{r^2-z^2}}\, dz. \qquad (2)$$

This results in the total surface of the solid as $16r^2$. If we compare this value with the surface area of a sphere ($4\pi r^2$), the solid resembles a sphere with radius of $\frac{\sqrt{\pi}}{2}r$. By increasing the number of cylinders, the intersection is increasingly spherical; for example in Figure 6 the result of intersecting ten cylinders is shown.

The 3-D structure of a shell cannot be realized with solid cylinders. To create a spherical shell, the cylinders must be hollow. The proposed method of creating a hollow cylinder is to use the pencil beam of the SARRP to trace the points on the surface of the cylinder. This is feasible because the SARRP has five degrees of freedom. The path for the beam is simply given by the equations of a 2-D circle in 3-D:

$$x^2+y^2 = r^2 \quad \texttt{(gantry at 0°)} \qquad (3)$$
$$y^2+z^2 = r^2 \quad \texttt{(gantry at 90°)} \qquad (4)$$

and by moving the robot X, Y and Z stages, the beam will paint the surface of a cylinder. For other gantry angles the equation should be transformed to the corresponding plane. In this method, the size of the sphere is limited by the stages' range of motion, which are designed to consider the requirements of small animal radiation. The output dose of the system is a direct function of the collimator and the robot speed. For a 1 mm pencil beam, the output dose is measured to be 2 Gy/min.

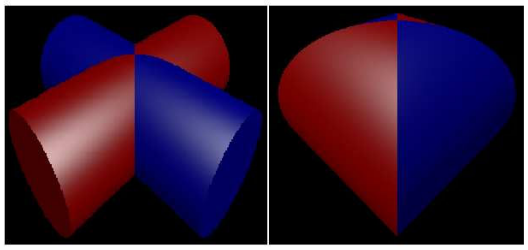

Fig. 5. Intersection of two right circular cylinders and the resulting volume known as Steinmetz solid. (Image courtesy of Wolfram MathWorld)

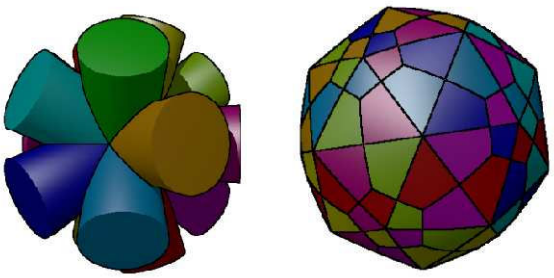

Fig. 6. Intersection of ten circular cylinders and the resulting volume that resembles a sphere. (Image courtesy of Wolfram MathWorld)

VI. Results

Gafchromic EBT film (International Specialty Products, Wayne, NJ) is used for dosimetric measurements. It has been shown that EBT film is ideal for two-dimensional (2-D) dose measurements at lower energies because of its energy independence and high sensitivity [14]. These films are composed of radiation sensitive polymers that cross link when exposed to radiation, visually appearing as dark spots on the film. For dosimetry measurements, EBT films are scanned three times pre and post radiation and uploaded into a Matlab program for calculation of the dose distribution across the film. The program subtracts pre irradiation films

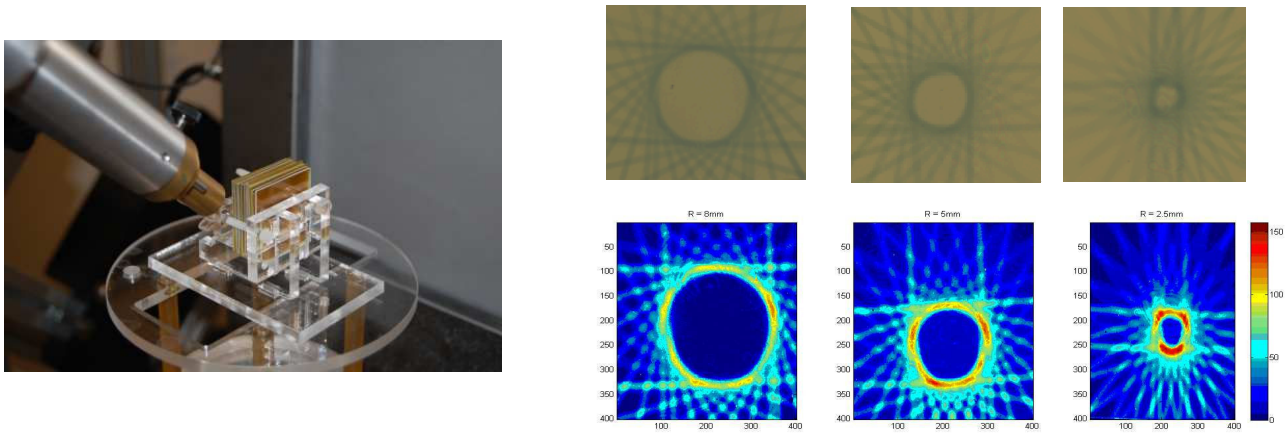

Fig. 7. The phantom consisting of a stack of EBT films used to illustrate the intersection of a dose shell and a plane (EBT films) - left , and intersections of the EBT film planes and the spherical dose shell with different radii and the corresponding dose images - right

from the post irradiation scans, and converts pixel values to dose via a calibration curve established with a ^{60}Co source. To simulate realistic testing conditions, the films are sandwiched between 1 mm-thick tiles of Acrylic plastic (a better choice is water-equivalent plastic), as shown in Figure 7-left.

To be able to target a full circular shell, beams are delivered to the film phantom from the seven gantry angles when the rotary stage is at 0° and 180°. The results indicated that a 1 mm beam produced a well-defined shell, where the maximum dose is delivered to the perimeter, Figure 7-right. The area inside the shell received no dose. All beams overlapped over the edge of the shell and created a circular shape receiving a maximum dose of 249.8 cGy in 4 min. The beam was hardened by a 0.25 mm Cu filter and the source to surface distance (SSD) was 35 cm. More precise contours can be generated using smaller size beams (e.g. 0.5 mm), however the effective dose will drop sharply. Output dose may be increased by decreasing beam filtration or by decreasing the SSD.

The procedure in the previous section is extended to create contours of different organ shapes, such as a mouse brain. The 3-D structure of interest is first defined in Pinnacle [15] [1]. MR/CT scans of the mouse brain are used to identify the 3-D structure in each slice, which is then contoured. These contours are combined to create a 3-D triangular mesh, which represents all surface and volumetric features of the structure. Pinnacle can visualize 3-D mesh objects from a beams eye view (BEV), and use this facility to project a 2-D shape corresponding to a particular gantry angle, as shown in Figure 8. The software uses the projection to create a "blocking mask" which can be written to an ASCII file. Once this beam shape is defined and extracted, it must be converted into a trajectory that can be executed by the robot. This path is stored in an ASCII file, and loaded by

[1]Pinnacle is a radiation therapy planning system by Philips, capable of volumetric 3D image processing, multi modality image fusion and an intuitive plan modification and optimization environment

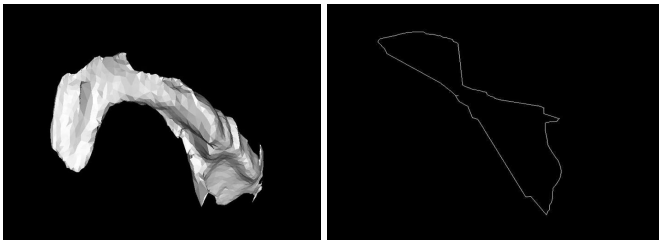

Fig. 8. The 3-D structure of left lateral ventricle defined in Pinnacle (left) and the corresponding projection contour from a beam eye views at gantry angle 45° (right).

the robot software, which navigates sequentially to each point using the robotic motion functions. The contour generated from the cutting algorithm is represented on the XY plane, but in order to dose paint on the SARRP, it must be aligned perpendicular to the gantry angle of interest using coordinate transformations. Figure 9 shows projection contours of the left lateral ventricle from multiple beams eye views and validation films showing contours with 0.5 mm collimators. The intersection of the contours from different gantry angles creates the 3-D mesh structure of the ventricle.

VII. Discussion and Future Work

The ability to deliver a dose shell allows mechanistic research of how a tumor interacts with its microenvironment to sustain its growth and/or lead to its resistance or recurrence. Clinically, it is also important to recognize that, in addition to the bulk tumor, its microenvironment is also a biological target. With dose shells, one can study how large is the biological target of the microenvironment, and how much dose is needed to have a therapeutic effect. It is possible that such a strategy allows the control of a tumor with considerably lower dose. The case in point is radiation surgery of brain tumors, where the entire tumor is irradiated. The standard practice is to give lower dose for larger tumors due to concerns about the large integral dose to the brain. Our current approach to treat these large tumors is a losing

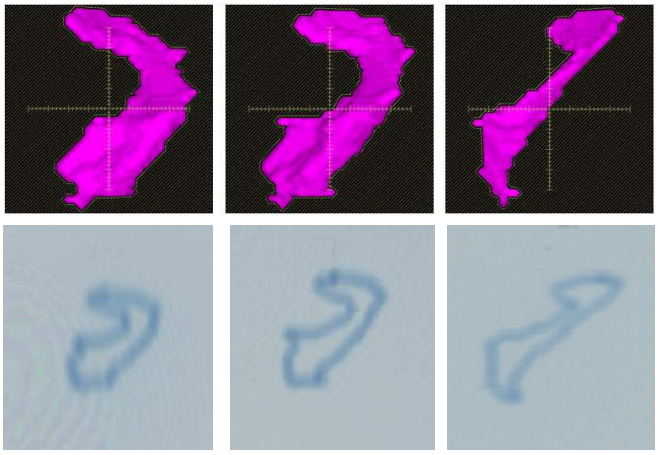

Fig. 9. Projection contours of the left lateral ventricle from multiple beams eye views (top) and validation films showing contours with 0.5 mm collimators (bottom).

proposition to begin with.

Shell dosimetry is also of interest to study the effect of radiation on neurogenic stem cells. These stems cells can play a role in repairing cognitive functions damaged by radiation therapy. They reside in a small niche surface of the mouse ventricles, a generalized form of shell. The ability to irradiate these shell type target regions while limiting dose to other regions would be highly desirable to study dose response of the stem cells, their transformation and their migratory paths, uncomplicated by the damage to the surrounding regions. Note that these studies cannot be performed in humans. The hypotheses must be tested in pre-clinical animal studies before translating to human applications.

In this paper, we presented a novel system for small animal radiation with advanced imaging and irradiation capabilities that mimics methods employed in modern human treatment. Moreover, we introduced a procedure that enables the SARRP to create a dose shell on phantom films from multiple gantry angles. By directing the 1 mm pencil beam at each of 7 gantry angles from vertical to horizontal, 19 right circular dose cylinders were delivered by a combination of translation (x,y,z) stages and rotation $(0^\circ, 90^\circ, 180^\circ)$ stage. The intersection of these open cylindrical dose shells formed a 1 mm wide "closed" spherical dose shell with a diameter of 8mm. Upon creating the shell, therapeutic dose surrounds the target volume and disrupts the blood supply to the tumor. As compared to whole tissue radiation therapy, shell dose distribution can minimize the total amount and time of radiation exposure.

The future work will be aimed at creating more complex shells. At this moment, we are able to create any contour for different organ shapes using the SARRP. The exact shape of the intersection mesh is a subject of further research. We are considering a transparent gel phantom to better illustrate the contours and their intersections. Gel dosimetry is commonly used to optically measure the shape of dose and scanned in 3-D to extract quantitative dose. Small animal experiments will be performed to study, validate and quantify the procedure.

VIII. ACKNOWLEDGMENTS

This work is supported by NIH R01 CA108449. We thank Eric Ford, Santosh Iyer, Eric Tryggestad, Elwood Armour, and Michael Armour for their contributions to this project.

REFERENCES

[1] J. Wong, E. Armour, P. Kazanzides, I. Iordachita, E. Tryggestad, H. Deng, M. Matinfar, C. Kennedy, Z. Liu, T. Chan, O. Gray, F. Verhaegen, T. McNutt, E. Ford, and T. L. Deweese, "High-resolution, small animal radiation research platform with x-ray tomographic guidance capabilities," *International Journal of Radiation Oncology, Biology and Physics*, vol. 71, no. 5, pp. 1591–1599, Aug 2008.

[2] P. Lindsay, S. Ansell, D. Moseley, S. Jelveh, R. Hill, and D. Jaffray, "Development of an image-guided conformal small animal irradiation platform," *Journal of Medical Physics*, vol. 35, no. 6, pp. 2695–2695, June 2008.

[3] S. Wang, Z. Liu, S. Sultana, E. Schreiber, O. Zhou, and S. Chang, "A novel high resolution micro-radiotherapy system for small animal irradiation for cancer research," *Journal of BioFactors*, vol. 30, pp. 265–270, 2007.

[4] S. Stojadinovic, D. Low, A. Hope, M. Vicic, J. Deasy, J. Cui, D. Khullar, P. Parikh, K. Malinowski, E. Izaguirre, S. Mutic, and P. Grigsby, "MicroRT-small animal conformal irradiator," *Journal of Medical Physics*, vol. 34, no. 12, pp. 4706–4716, Dec 2007.

[5] E. Graves, H. Zhou, R. Chatterjee, P. Keall, S. Gambhir, C. Contag, and A. Boyer, "Design and evaluation of a variable aperture collimator for conformal radiotherapy of small animals using a microCT scanner," *Journal of Medical Physics*, vol. 34, no. 11, pp. 4359–4367, Nov 2007.

[6] M. Brown, G. Ahn, and M. Kioi, "The influence of bone marrow derived cells in tumor radiosensitivity," in *Proc. 4th International Conference on Translational Research, Radiotherapy and Oncology*, Sept. 2009, pp. s17–s18.

[7] T. Apostol and M. Mnatsakanian, "Solids circumscribing spheres," *Journal of American Mathematics*, vol. 6, pp. 521–540, 2006.

[8] M. Matinfar, E. Ford, I. Iordachita, J. Wong, and P. Kazanzides, "Image-guided small animal radiation research platform: calibration of treatment beam alignment," *Journal of Physics in Medicine and Biology*, vol. 54, pp. 891–905, 2009.

[9] L. Feldkamp, L. Davis, and J. Kress, "Practical cone-beam algorithm," *Optical Society of America*, vol. A, no. 1, pp. 612–619, 1984.

[10] M. V. Herk, A. Betgen, B. Brand, D. Jaffray, P. Remeijer, M. Smitsmans, J. Sonke, and L. Zijp, "An integrated system for on-line cone-beam ct image-guided radiotherapy software aspects," in *Proc. 14th International Conference on the Use of Computers in Radiation Therapy*, May 2004.

[11] G. T. Herman and W. Chena, "A fast algorithm for solving a linear feasibility problem with application to intensity-modulated radiation therapy," *Linear Algebra and its Applications*, vol. 428, pp. 1207–1217, 2008.

[12] M. Matinfar, S. Iyer, E. Ford, J. Wong, and P. Kazanzides, "Image guided complex dose delivery for small animal radiotherapy," in *Proc. 6th International Symposium on Biomedical Imaging*, June 2009, pp. 1243–1246.

[13] Y. Censor, J. M. Galvin, Y. Xiao, and M. Langer, "Linear and nonlinear models and algorithms in intensity-modulated radiation therapy," *Linear Algebra and its Applications*, vol. 428, pp. 1203–1206, 2008.

[14] S. Devic, J. Seuntjens, E. Sham, E. Podgorsak, C. Schmidtlein, A. Kirov, and C. Soares, "Precise radiochromic film dosimetry using a flat-bed document scanner," *Journal of Medical Physics*, vol. 32, pp. 2245–53, 2005.

[15] T. McNutt, "Dose calculations - collapsed cone convolution superposition and delta pixel beam," *Philips Medical Systems, www.medical.philips.com/main/products/ros/products/pinnacle3/.*